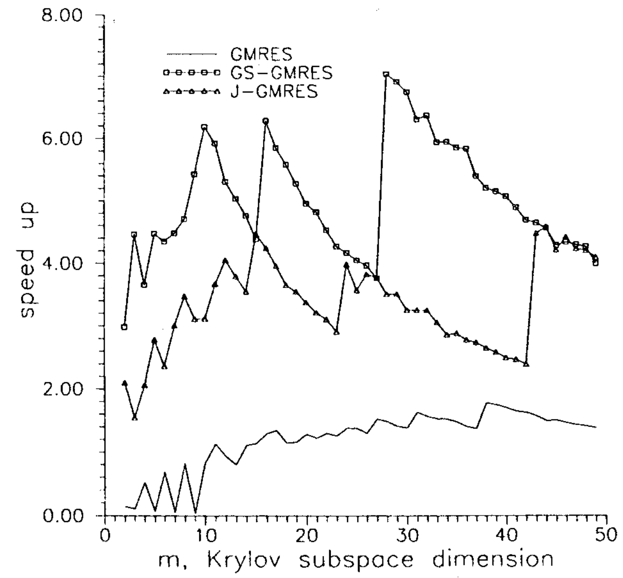

Fig. 2 Comparison of speed up of the three schemes (aircraft case).

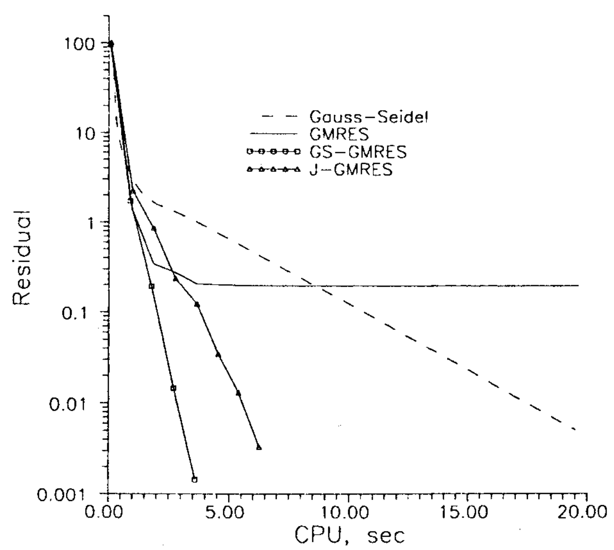

Fig. 3 Convergence history (m = 9, aircraft) with and without preconditioners.

responding figures are different for the two test cases. With the wing case, the best speed up is about 4 and the average speed up is about 2.8. The corresponding figures are about 1.8 and about 1.4, respectively, for the aircraft case.

It may be seen in Fig. 2 that for certain dimensions of the Krylov subspace, GMRES (without preconditioner) does not converge. Such cases are not observed in Fig. 1, for the wing-alone case. This may be due to the fact that the ordering of the panels in the aircraft case is arbitrary. In the wing case, panels are ordered stripwise. Structured panels would lead to some structure in the matrix also.

The convergence histories for the three GMRES schemes and point Gauss–Seidel iteration scheme are compared in Fig. 3, for a case where GMRES does not converge (m = 9). There is no convergence problem with either GS-GMRES or J-GMRES.

Conclusions

It has been shown in the present study that preconditioned GMRES is very efficient in obtaining solutions to linear systems with fully populated matrices arising in panel methods. GMRES with Gauss–Seidel preconditioner performs the best. It gives maximum speed ups (over Gauss–Seidel iterations) of about 7, and average speed ups of the order of 5, with panel method matrices. Jacobi preconditioner is also effective, but the corresponding speed ups obtained are less, about 5 and 3, respectively.

Acknowledgment

The author thanks his colleague Biju Uthup, who introduced him to Krylov subspace methods.

References

[1]Bristow, D. R., and Hawk, J. D., "Subsonic Panel Method for Designing Wing Surfaces from Pressure Distribution," NASA CR-3713, July 1983.

[2]Hawk, J. K., and Bristow, D. R., "Subsonic Surface Panel Method for Airframe Analysis and Wing Design," AIAA Paper 83-0341, Jan. 1983.

[3]Johnson, F. T., "A General Panel Method for the Analysis and Design of Arbitrary Configurations in Incompressible Flows," NASA CR-3079, May 1980.

[4]Magnus, A. E., and Epton, M. A., "PAN AIR—A Computer Program for Predicting Subsonic or Supersonic Linear Potential Flows About Arbitrary Configurations Using a Higher Order Panel Method," NASA CR-3251, April 1980.

[5]Saad, Y., and Schultz, M. H., "GMRES: A Generalised Minimum Residual Algorithm for Solving Nonsymmetric Linear Systems," *SIAM Journal of Scientific and Statistical Computing*, Vol. 7, No. 3, 1986, pp. 856–859.

[6]Koruthu, S. P., "GMRES Acceleration of Subsonic Panel Methods," *Journal of the Aeronautical Society of India* (submitted for publication).

[7]Sudhakar, K., Koruthu, S. P., and Shevare, G. R., "3D Wing Analysis Using a Low Order Panel Method," *Journal of the Aeronautical Society of India*, Vol. 38, No. 4, 1986, pp. 303–306.

[8]Boersen, S. J., and Elsenaar, A., "Tests on the AFWAL 65° Delta Wing at NLR: A Study of Vortex Flow Development Between Mach = 0.4 and 4," *Proceedings of the Symposium on International Vortex Flow Experiment on Euler Code Validation*, 1986, FFA, Bromma, Sweden, pp. 23–36.

Effect of Canard Oscillations on an X-31A-Like Model in Pitching Maneuver

Sheshagiri K. Hebbar,* Max F. Platzer,† and Da-Ming Liu‡

Naval Postgraduate School, Monterey, California 93943-5000

Introduction

THE favorable interference effect between the vortex systems of the static canard and the wing in a close-coupled canard configuration has been well recognized and demonstrated.[1,2] Another potential area of interest for lift enhancement involves interaction between an oscillating close-coupled canard and the flowfield of the main wing. During canard

Presented as Paper 93-3427 at the AIAA 11th Applied Aerodynamics Conference, Monterey, CA, Aug. 9–11, 1993; received May 15, 1994; revision received March 21, 1995; accepted for publication April 4, 1995.

*Adjunct Professor, Department of Aeronautics and Astronautics. Associate Fellow AIAA.

†Professor, Department of Aeronautics and Astronautics. Associate Fellow AIAA.

‡Currently, Lieutenant Commander, Republic of China Navy.

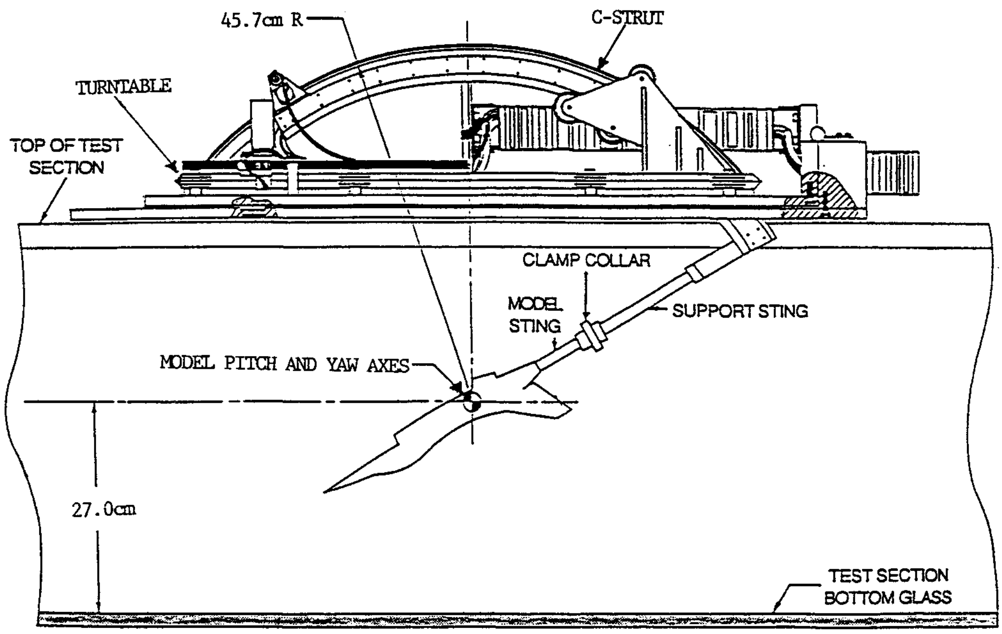

Fig. 1 Model support system of the NPS water tunnel.

oscillations, the canard tip vortex and the canard wake become unsteady. In addition, the dynamic stall vortex shed from canard's leading edge plays a role in modifying the wing flowfield. The interaction during the dynamic motion of the wing becomes even more complicated as it is influenced by additional parameters defining the dynamic motion. The experimental data available on the influence of canard oscillations on the flow characteristics of the static wing are limited,[3-5] and the data for the dynamic case are still rather scarce, even for simple wing shapes, let alone for complete aircraft configurations.[6,7] The objective of this investigation therefore was to study the influence of an oscillating canard on an X-31A-like model in both static and dynamic (pitching) conditions. Specifically, the wing root vortex breakdown characteristics were investigated in the Naval Postgraduate School (NPS) water tunnel using the dye-injection technique. The data reported here is believed to be the first of its kind for an oscillating canard-configured model in pitching motion. These results should be of interest to researchers working on similar configurations, especially in view of the clean support system used. Additional details of the investigation appear in Refs. 8 and 9.

Experimental Program

The NPS water tunnel is a horizontal, continuous-flow, closed-circuit facility with a test section 38 cm wide, 51 cm high, and 152 cm long.[8,9] The model support system attached to the top of the tunnel (Fig. 1) has two servomotors providing independent control of model pitch and yaw. The X-31A-like model used in this investigation is a simplified 2.3% scale model resembling the Navy's X-31A fighter demonstrator with a double-delta wing, a close-coupled delta-canard, and a rectangular fuselage (Fig. 2). While the wing section has a NACA 66-206 profile, the canard is essentially a flat plate airfoil with square leading edges. Dye injection is accomplished through dye tubes located on the bottom surface of the wing close to the fuselage. Some key model dimensions are shown in Fig. 2. The canard can be oscillated at two frequencies by a flexible shaft driven by a small dc motor through a speed reduction gear unit. With the mean-deflection angle of the canard δ set at 0 deg, the canard amplitude δ_a can be varied up to ± 25 deg.

The program was carried out in two phases with zero sideslip, the first phase involving the static model at different angle

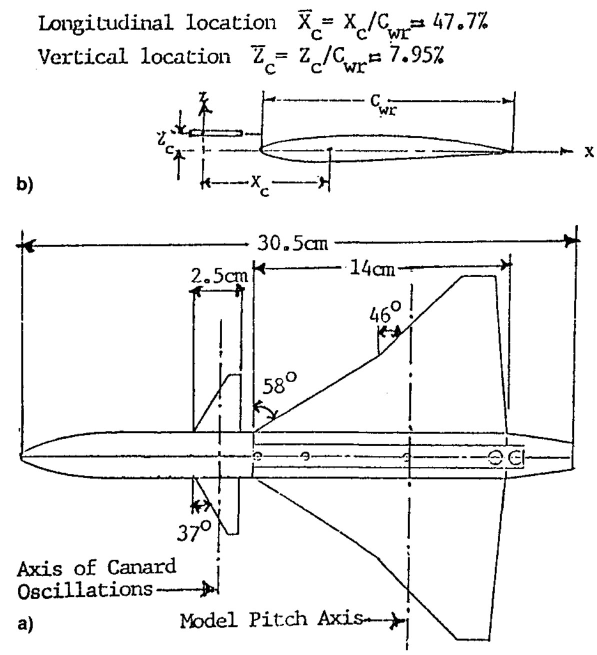

Fig. 2 X-31A-like aircraft model: a) model planform and b) canard location (schematic).

of attacks (AOAs) and the second phase involving the dynamic model executing simple pitch-up and simple pitch-down motions in the AOA range α = 0–50 deg. The flow velocity was 7.6 cm/s, corresponding to a nominal Reynolds number of 10.2×10^3 based on the wing root chord C_{wr}. The reduced pitch rates were $k = \dot{\alpha}L/2U_\infty = 0.08$ and 0.16, where L is the model length, U_∞ is the freestream velocity, and $\dot{\alpha}$ is the pitch rate in rad/s. The model pitch axis was located at 62.7% of the wing root chord. The canard reduced frequency parameters were $k_c = \omega C_{cr}/2U_\infty = 1.7$ and 10.4, where C_{cr} is the canard root chord and ω is the canard oscillation frequency in rad/s. The canards were oscillating about a lateral axis passing through the midpoint of the root chord. Extensive videotape recording and 35-mm photography of the model flowfield in both top and side views were performed to document the observed flow phenomena.

Results and Discussion

All measurements were made on the starboard side, with the streamwise burst location of the wing root vortex X_b referenced from the leading edge of the wing root chord. For the dynamic case (with either the model pitching or the canard oscillating) the video playback was used extensively for measurements. The determination of burst location was impossible in the case of high-frequency, large-amplitude canard oscillations because of the intermittent nature of the vortex core and the spreading of the dye. During the static segment of the experiment, the burst location fluctuated as much as ± 6.3 mm (about $\pm 4.5\%$ of the wing root chord).

Figure 3 shows the effect of positive and negative canard deflection on the wing root vortex breakdown as a function of AOA. These plots clearly highlight the unfavorable interaction (earlier bursting) caused by positive or negative deflection angle of the canard. The canard in this investigation is a flat plate airfoil with a square leading edge, and therefore, the flow over and under it is very likely separated at any deflection setting. It is therefore not surprising that the interaction of the canard tip vortex field and the canard wake flowfield with the flow over the upper surface of the wing does not lead to any beneficial results. Figure 4 illustrates the effect of canard oscillations on the vortex burst location as a function of AOA. Also shown here for comparison is the burst location plot corresponding to the static model with the static canard. It is clear that the small-amplitude, low-frequency oscillations tend to destabilize the vortex core, i.e., cause early vortex bursting, whereas the small-amplitude, hf oscillations appear to have a favorable interaction with the vortical flowfield resulting in a somewhat delayed vortex bursting. Note that the large-amplitude, lf oscillations result in a marginally favorable interaction. Figures 5–7 illustrate the effect of canard oscillations on the vortex burst location as a function of AOA during pitching motions. For the sake of comparison, the appropriate burst plots for the dynamic model with the static canard are also included in each of these figures. The results are summarized as follows:

1) Small-amplitude, lf canard oscillations can lead to beneficial interaction with the wing vortical flowfield during low pitch rate, but may adversely interact during high pitch rate.

2) Small-amplitude, hf canard oscillations can adversely affect the wing vortical flowfield during pitching motions in general.

3) The large-amplitude, lf oscillations lead to favorable interaction of the wing vortical flowfield at high AOAs during up or down pitching motions.

The overall integrated dynamic effect of the small-amplitude, lf canard oscillations ($\delta_a = \pm 5$ deg, $k_c = 1.7$) on the static wing leads to destabilization of the wing vortex core (early vortex bursting) and is essentially the same as that produced by an equivalent static deflection angle of the canard, suggesting that the canard's resulting unsteady flowfield

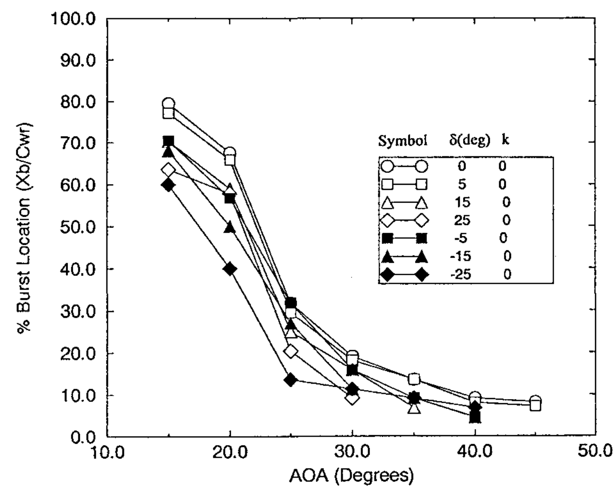

Fig. 3 Wing root vortex burst location for static model with positive and negative canard deflection angles.

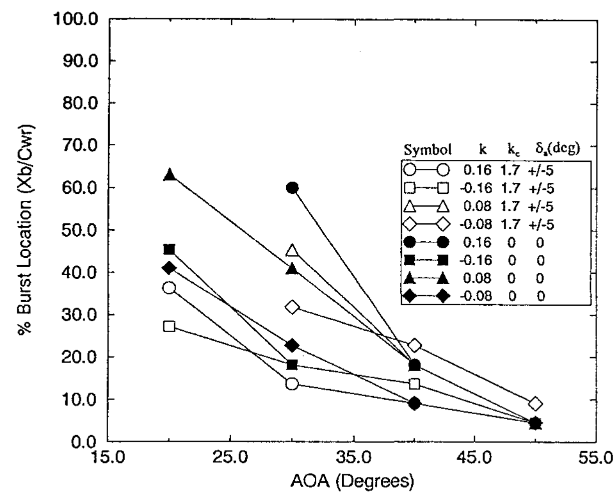

Fig. 5 Wing root vortex burst location for pitching model with oscillating canard.

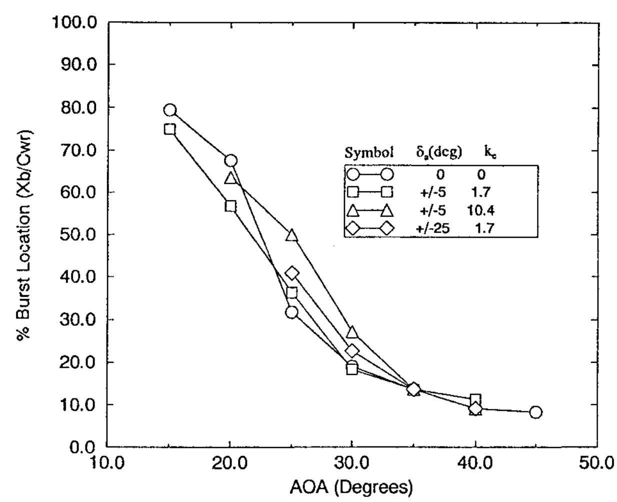

Fig. 4 Wing root vortex burst location for static model with oscillating canard.

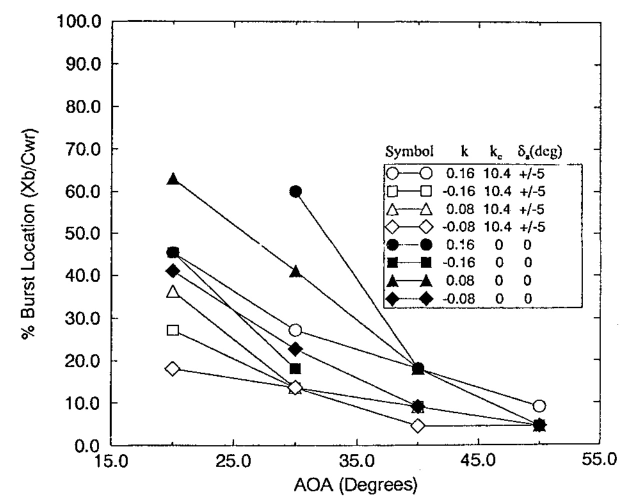

Fig. 6 Wing root vortex burst location for pitching model with oscillating canard.

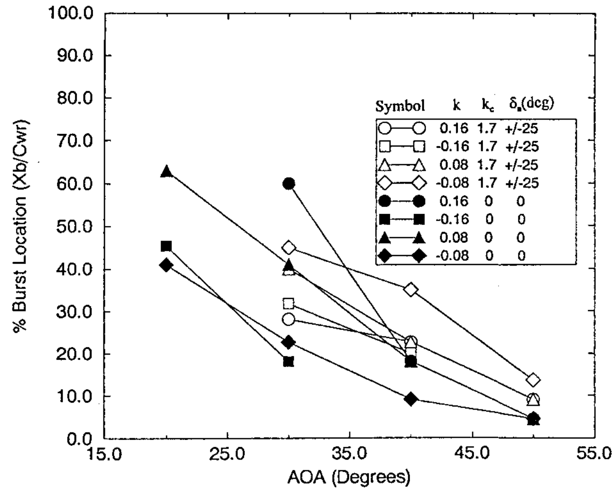

Fig. 7 Wing root vortex burst location for pitching model with oscillating canard.

at low frequencies behaves more like a slowly varying field with negligible unsteady effects. However, with increase in the frequency ($\delta_a = \pm 5$ deg, $k_c = 10.3$), the integrated dynamic effect leads to stabilization of wing vortex core (delayed vortex bursting), which is in contrast to the effect of the static canard deflection angle. This points to possible potential benefits of using canard oscillations for controlling the wing flowfield. The interaction can be quite different during the dynamic motion of the model, with pitch rate influencing the interaction. Indeed, the present data indicate that the large-amplitude, lf oscillations of the canard have negligible influence on the vortical flowfield of the static model, but lead to favorable interactions on the pitching model, particularly at high AOAs.

Conclusions

Static Model

At small amplitude, the lf canard oscillations tend to destabilize the wing vortex core (early bursting), whereas the hf oscillations delay vortex bursting. The large-amplitude, lf oscillations seem to have a marginally favorable effect on the wing vortical flowfield.

Dynamic Model

The dynamic tests indicate that the large-amplitude, lf oscillations of the canard interact favorably with the wing vortical flowfield to delay vortex bursting during pitch-up or pitch-down motion.

Acknowledgments

This work was supported by the Naval Air Warfare Center/Aircraft Division, Warminster, Pennsylvania, the Naval Air Systems Command and the Naval Postgraduate School. The authors sincerely thank Alan McGuire for helping in the design and fabrication of the model.

References

[1]Behrbohm, H., "Basic Low Speed Aerodynamics of the Short-Coupled Canard Configuration of Small Aspect Ratio," SAAB Aircraft Co., TN-60, Linkoping, Sweden, July 1965.

[2]Hummel, D., and Oelker, H., "Effects of Canard Position on the Aerodynamic Characteristics of a Close-Coupled Canard-Configuration at Low Speed," AGARD CP 465, Oct. 1989, pp. 7.1–7.18; also *Journal of Aircraft*, Vol. 26, No. 7, 1989, pp. 657–666.

[3]Ashworth, J., Mouch, T., and Luttges, M., "Visualization and Anemometry Analyses of Forced Unsteady Flows About an X-29 Model," AIAA Paper 88-2570, June 1988.

[4]Mouch, T., McLaughlin, T., and Ashworth, J., "Unsteady Flows Produced by Small Amplitude Oscillations of the Canard of an X-29 Model," AIAA Paper 89-2229, July/Aug. 1989.

[5]Huyer, S. A., and Luttges, M. W., "Unsteady Flow Interactions Between the Wake of an Oscillating Airfoil and a Stationary Trailing Airfoil," AIAA Paper 88-2581, June 1988.

[6]Hebbar, S. K., Platzer, M. F., and Kwon, H. M., "Vortex Breakdown Studies of a Canard-Configured X-31A-Like Fighter Aircraft Model," *Journal of Aircraft*, Vol. 30, No. 3, 1993, pp. 405–408.

[7]Hebbar, S. K., Platzer, M. F., and Kim, C. H., "Experimental Investigation of Vortex Breakdown over a Sideslipping Canard-Configured Aircraft Model," *Journal of Aircraft*, Vol. 31, No. 4, 1994, pp. 998–1001.

[8]Liu, D. M., "Effect of Canard Oscillations on the Vortical Flowfield of a X-31A-Like Fighter Aircraft Model," M.S. Thesis, Naval Postgraduate School, Monterey, CA, March 1992.

[9]Hebbar, S. K., Platzer, M. F., and Liu, D. M., "Effect of Canard Oscillations on the Vortical Flowfield of an X-31A-Like Fighter Model in Dynamic Motion," *Proceedings of the AIAA 11th Applied Aerodynamics Conference*, 1993, pp. 241–250 (AIAA Paper 93-3427).

Effects of Delta Planform Tip Sail Incidence and Arrangement on Wing Performance

Lance W. Traub*
University of the Witwatersrand, Johannesburg, South Africa

Nomenclature

C_D = drag coefficient
C_L = lift coefficient
C_m = pitching moment coefficient
ds = sail incidence, defined positive following a nose-down deflection
α = angle of attack

Introduction

NUMEROUS wingtip devices have been investigated to attenuate vortex drag. These encompass apparatus to reduce drag by releasing trailing vorticity over a substantial vertical distance (e.g., endplates[1] and winglets[2,3]), as well as essentially planar devices (e.g., tip sails[4,5] and various forms of spanwise blowing,[6,7] etc.). Generally, any induced drag benefits accruing from vorticity attenuation on an end plate are usually mitigated by interference drag.[8] Winglets have proved to be successful, but require careful design and implementation.[2,3] Blowing[6,7] may improve performance essentially through increasing the wings' aspect ratio (AR),[7] but does introduce the complexity of ducting and air required to operate the system.

In an earlier preliminary investigation,[5] the delta planform tip sail was cited as a simple device to improve wing performance, and avoid complications associated with winglet implementation. This was essentially due to the delta planform tip sail not requiring attached flow, and having reduced sensitivity to Reynolds number. The study included variation of the sails leading-edge sweep angle and its taper ratio. How-

Received March 16, 1995; revision received April 4, 1995; accepted for publication April 5, 1995.

*Graduate Student, School of Mechanical Engineering, Branch of Aeronautical Engineering, 1 Jan Smuts Ave., P.O. Wits, 2050; currently at Texas A&M University, College Station, TX 77840.